

# Application of Bingham statistics to a paleopole data set: Towards a better definition of APWP trends?

D.P. Cederquist, C. Mac Niocaill, R. Van der Voo \*

*Department of Geological Sciences, The University of Michigan, Ann Arbor, MI 48109-1063, USA*

Received 11 June 1996; revised 17 September 1996; accepted 21 October 1996

---

## Abstract

Bingham statistical analyses were applied to paleomagnetic data from 50 published studies from North America, of Carboniferous through Early Jurassic age, in an attempt to test whether the azimuths of the long axes of the Bingham ellipses lie tangent to the apparent polar wander path. The underlying assumption is that paleomagnetic directions will form a Fisherian (circular) distribution if no apparent polar wander has taken place during magnetization acquisition. However, the distribution should appear elongated (elliptical) if magnetization acquisition occurred over a significant amount of time involving apparent polar wander. The long axes in direction space yield corresponding azimuths in paleopole space, which can be compared to the North American APWP. We find that, generally, these azimuths are indeed sub-parallel to the APWP, validating the methods and the hypothesis. Plotting a pole as an azimuthal cord, representing the long axis of the ellipse, will provide additional robustness or definition to an APWP based upon temporally sparse paleomagnetic studies.

*Keywords:* paleomagnetism; North America; apparent polar wandering; pole positions

---

## 1. Introduction

For more than four decades, paleomagnetic studies have been used to determine the paleolatitudes and orientations of continents. By connecting paleopole positions through time relative to the current continental position, apparent polar wander paths (APWPs) have been developed for each major continent for much of Phanerozoic time. The APWPs for the different continents, however, are of variable quality and are occasionally based on sparse data

sets or on results with poor age constraints. When paleopole locations are few and far between, paleomagnetists have had no choice but to connect the poles by straight lines, which at best may reflect a highly smoothed path (Fig. 1a). In addition, if the ages of the poles are poorly known, the younging direction of the path may be poorly constrained.

Paleomagnetic poles are typically plotted with a 95% confidence oval based upon a presumably circular (Fisherian) statistical distribution of the paleomagnetic directions [1]. The distribution of directions will be circular if errors in sample orientation, structural bedding determination and laboratory measurements are randomly distributed. Departures from cir-

---

\* Corresponding author. E-mail: voo@umich.edu

Table 1  
Summary of Carboniferous–Triassic paleomagnetic data from North America used in our analysis

Rock unit	Dec	Inc	Site lat.	Site long.	Az	$\alpha_{1-3}$	$\alpha_{1-2}$	$\alpha_n$	N	$\theta$	Reference
Kayenta Fm., AZ	1.1	9.9	36.0	248.7	14.8	2.6	3.6	1.4	23	< 5°	[8]
Owl Rock Member (High T), NM	2.3	6.3	36.5	250.6	14.3	2.8	3.5	1.3	18	< 5°	[8]
Owl Rock Member (Micrite), NM	359.4	28.4	36.5	250.7	167.3	2.5	4.1	1.7	9	< 5°	[8]
Upper Shale Member, NM	355.2	4.9	35.0	256.1	102.3	4.2	6.9	1.6	16	65–70°	[8]
Joggins section, Nova Scotia	354.7	-14.2	45.7	295.5	35.3	2.2	4.1	1.8	10	5–10°	[6]
Piedmont Dykes, GA, SC, NC	4.7	24.9	34.4	278.5	70.4	6.5	9.1	1.4	15	30–35°	* Dooley and Smith, 1982
Moenave Fm., AZ	7.5	11.1	36.9	247.2	157.9	4.5	6.4	1.4	23	30–35°	* Ekstrand and Butler, 1989
Viola Limestone, OK (unmineralized)	320.7	-10.1	34.4	262.8	55.2	4.1	8.2	2.0	14	5–10°	[9]
Abbott Pluton, ME	10.9	5.8	43.5	289.1	94.3	2.0	3.8	1.9	7	25–30°	* Fang and Van der Voo, 1988
Agamenticus Pluton, ME	7.0	4.1	43.2	289.2	62.8	1.9	3.2	1.7	9	< 5°	* Fang and Van der Voo, 1988
Cutler Fm., UT	329.5	3.8	38.4	250.4	153.5	1.5	3.0	2.0	31	85–90°	* Gose and Helsley, 1972
Moenkopi Fm., CO	352.0	12.3	38.6	251.1	75.0	3.9	7.4	1.9	6	25–30°	* Helsley, 1969
Upper Moenkopi Fm., CO	341.4	14.7	38.6	251.1	80.4	3.7	5.5	1.5	7	40–45°	* Helsley and Steiner, 1974
Chugwater Fm., WY	335.3	15.9	43.4	250.6	87.1	3.9	6.7	1.7	6	35–40°	* Herrero-Bervera and Helsley, 1983
North Mountain Basalt, NB	18.0	45.0	45.5	295.5	176.1	5.5	11.8	2.2	9	25–30°	* Hodych and Hyatsu, 1988
Mauch Chunk Fm., PA	340.8	-27.2	40.6	282.9	78.5	6.3	8.4	1.3	23	15–20°	* Kent and Opdyke, 1985
Newark Basin drillcores	3.4	13.2	40.4	283.4	25.9	0.9	4.5	5.0	7	5–10°	[10]
Pz remag, Trenton LS, NY, Ont., Que.	347.8	18.8	44.4	284.6	60.4	3.8	4.6	1.2	8	15–20°	* McCabe et al., 1984
Watching Basalts, NJ, PA	7.7	28.4	40.8	285.6	166.7	4.2	7.0	1.7	18	5–10°	* McIntosh et al., 1985
Chimle Fm., NM	352.0	12.7	34.8	253.5	172.2	3.0	4.1	1.4	18	30–35°	* Molina-Garza et al., 1991
Tecovas Fm., TX	2.6	9.2	34.8	258.4	79.8	3.7	5.6	1.5	20	55–60°	[11]
Trujillo Fm., TX	346.2	1.5	34.7	258.6	95.4	8.1	12.8	1.6	6	5–10°	[11]
NJ Volcanics, NJ	3.1	26.9	40.6	285.3	117.9	5.0	7.4	1.5	11	< 5°	* Opdyke, 1961
MVT Ore B comp., AR and Tri-State	322.5	-19.4	37.5	265.5	3.2	7.8	13.0	1.7	7	50–55°	[13]
MVT Ore C comp., AR and Tri-State	340.2	-0.8	36.1	267.6	83.0	4.7	10.0	2.1	14	20–25°	[13]
Gays River ores, Nova Scotia	359.6	-13.0	45.1	296.7	98.4	2.5	6.3	2.5	16	55–60°	[14]
Pictou Red Beds, PEI	348.4	0.1	46.7	296.0	29.3	2.4	4.0	1.7	17	< 5°	[15]
Red Mtn. Fm., AL	331.4	-20.5	33.8	273.4	106.6	3.7	5.0	1.4	28	40–45°	[16]
Guadalupian Redbeds, NM, OK	332.6	9.9	34.2	257.7	127.7	3.5	6.2	1.8	7	35–40°	* Peterson and Nairn, 1971
Ochoan Redbeds, NM, OK	338.6	11.5	35.1	260.4	36.5	2.4	10.9	4.5	7	< 5°	* Peterson and Nairn, 1971
Bonaventure Fm., Quebec	345.9	-4.9	48.2	295.3	56.0	7.1	11.0	1.5	11	25–30°	* Roy, 1966
Red Beds, PEI	352.1	-2.2	46.5	296.6	113.8	3.5	8.8	2.5	20	60–65°	* Roy, 1966
Hurley Creek Fm., New Brunswick	351.4	-9.5	46.0	294.0	71.0	5.1	9.2	1.8	5	35–40°	* Roy et al., 1968
Cumberland Group, Nova Scotia	351.8	-15.4	45.7	295.6	164.3	3.8	5.0	1.3	11	65–70°	* Roy, 1969
Riversdale Group, Nova Scotia	354.6	-14.5	45.8	295.6	10.5	3.8	5.8	1.5	8	15–20°	* Roy, 1977
Hopewell Group, New Brunswick	355.1	-26.9	45.7	295.4	116.5	3.8	16.9	4.4	15	15–20°	* Roy and Park, 1969
Kiaman overprint, NY, ONT	341.6	4.4	42.9	283.7	133.4	3.7	4.6	1.2	12	55–60°	[17]

Mason Creek, IL	329.3	-8.2	41.3	271.3	33.9	4.7	8.7	1.8	8	<5°	*Scotese, 1985
Helderberg carbonates, NY	344.9	10.0	42.6	285.4	165.5	1.9	2.6	1.4	18	70–75°	*Scotese, 1982
New Brunswick Volcanics II	340.1	-11.1	46.0	293.6	19.2	4.1	8.2	2.0	10	<5°	*Seguin and Fyffe, 1986
Piedmont dikes, NC	20.2	26.5	35.7	280.4	11.8	4.6	9.3	2.0	26	35–40°	*Smith, 1987
Perry Fm., ME, NB	348.2	-17.3	45.0	293.0	176.4	6.5	13.5	2.1	19	50–55°	[18]
Kayenta Fm., UT	0.0	20.3	38.6	250.3	65.3	4.0	6.9	1.7	7	75–80°	*Steiner and Helsley, 1974
L. Fundy Grp., Nova Scotia, NB	16.4	13.6	45.2	295.0	30.5	6.1	8.6	1.4	21	<5°	*Symons et al., 1989
Pictou Red Beds, PEI	353.7	-2.6	46.5	297.2	8.9	3.1	7.4	2.4	22	25–30°	*Symons, 1990
Central MO MVT host, MO	336.0	-18.9	38.5	267.5	171.2	4.6	9.4	2.1	13	50–55°	[19]
Central MO MVT ores, MO	331.6	-16.9	38.5	267.5	17.3	4.4	7.2	1.6	21	75–80°	[19]
Chugwater Fm., WY	334.0	15.5	42.6	251.3	97.0	3.8	6.4	1.7	8	30–35°	*Van der Voo and Grubbs, 1977
Hettangian Newark Red Beds, NJ	6.3	12.9	40.8	285.7	73.8	3.7	6.5	1.7	11	40–45°	*Witte and Kent, 1990
Upper Passaic Fm., PA	5.6	13.0	40.4	284.7	23.3	4.1	5.4	1.3	26	5–10°	[20]

Abbreviations are as follows: Dec/Inc = overall mean declination/inclination from each study; Site lat/Site long = mean latitude and longitude of the sampling area; Az = the azimuth of the long axis of the error ellipse;  $\alpha_{1-3}$  = length of semiminor axis of the error ellipse;  $\alpha_{1-2}$  = the length of the semimajor axis of the error ellipse;  $\alpha_n$  = the ratio of the semimajor and semiminor axes of the error ellipse; N = number of sites or stratigraphic levels used.  $\theta$  represents an estimate of the angular difference between the azimuth calculated from the Bingham statistics and the trend of the APWP at the point closest to the polar-cord. References marked with an asterisk (\*) are given in Van der Voo [5].

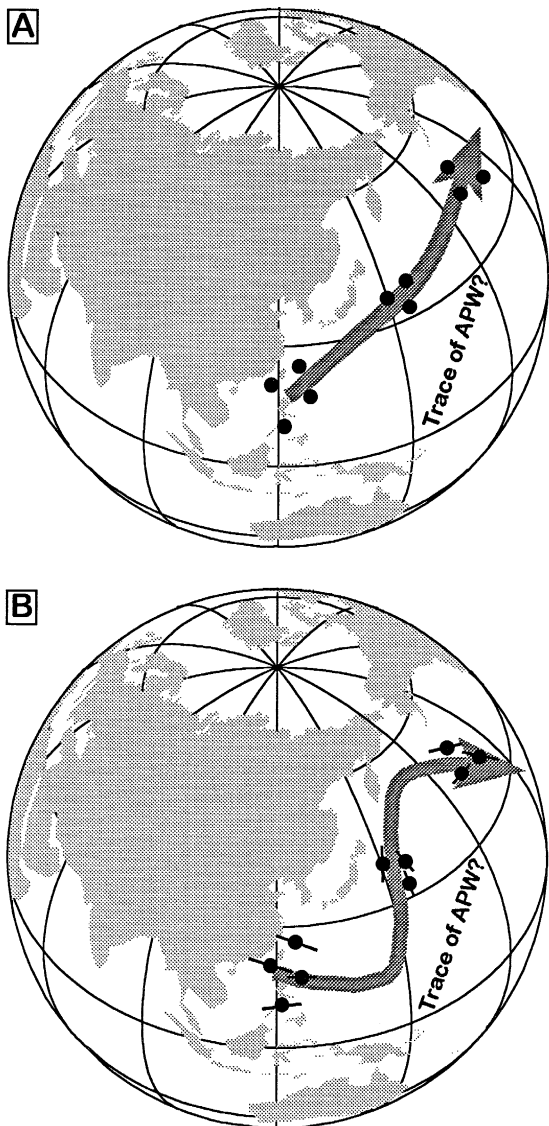


Fig. 1. (a) Schematic cartoon showing hypothetical clusters of poles of different ages with an APW path drawn through them. This essentially represents a smoothing of APW through time based on simply connecting successive clusters of poles. (b) The same clusters of poles but plotted with the azimuths of the Bingham error ellipse. Note how these provide extra resolution in elucidating the trend of the APW path.

cularity, on the other hand, can be caused by a systematic bias in the errors associated with the mean paleomagnetic direction, by incomplete removal of an overprint direction, or by sampling the geomagnetic field over such a long time that apparent polar wander is recorded in the directions. Bingham statistical analysis [2] evaluates the non-circularity (elongation) of a data set on a sphere and yields an ellipse of confidence around the mean direction; it has been recommended by Onstott [3] for the routine analysis of paleomagnetic data to evaluate the non-circularity of paleomagnetic directions attributable to random and non-random variation. If systematic bias or magnetic overprints are not apparent for a given result, any elongation in the data set can be attributed to APW [4] and the orientation of the long axis of the confidence ellipse is governed by the change in the paleofield direction over time.

We propose that the orientation of this long axis can be used in constructing APW paths. By projecting these orientations into polar co-ordinates we obtain tangential “cords” which yield the trend of APW for the time duration in question. Thus, the trend of the cords may resolve more detail in the APW path than is possible with conventional Fisher [1] statistics (Fig. 1b). To evaluate the validity and applicability of this technique we have performed the analysis on the Late Carboniferous–Early Jurassic North American paleomagnetic data in order to test the match between the cords and a well constrained APW path.

## 2. Analytical methods

The Late Carboniferous through Early Jurassic paleomagnetic studies used for the analyses are from Van der Voo [5], using results with a quality factor,  $Q$ , equal to or greater than 3, with more recent studies added and listed in Table 1. A majority of the

### Note to Table 2:

Data were rejected where less than five sites were available, if the magnetization was synfolding, since the resulting mean could be biased by the degree of unfolding used, if the alpha-ratio ( $\alpha_n$ ) was less than 1.2 (i.e. indicating a nearly circular distribution) or where no site or stratigraphic means (NSM) were presented in the original publication. References marked with an asterisk (\*) are given in Van der Voo [5].

Table 2  
Carboniferous–Early Jurassic data from North America not used in our analysis

Rock unit	Reason for rejection	Reference
Upper Moenkopi drillcore, CO	N < 5	* Baag and Helsley, 1974
Ordovician Carbonates, TN	syn-folding magnetization	* Bachtadse et al., 1987
Churchland Pluton, NC	NSM	* Barton and Brown, 1983
Conn. Valley volcanics, CT, MA	N < 5	* De Boer, 1968
Ingelside Fm., CO	NSM	* Diehl and Shive, 1979
Casper Fm., WY	NSM	* Diehl and Shive, 1981
Shepody Fm., Nova Scotia	NSM	* DiVenere and Opdyke, 1990
Maringouin Fm., Nova Scotia	NSM	* DiVenere and Opdyke, 1990
Piedmont Mafics, SC	mix of disparate ages	* Dooley, 1983
Hoskinnini Tongue, AZ	N < 5	* Farrell and May, 1969
Cutler Fm., UT	N < 5	* Gose and Helsley, 1972
Elephant Canyon Fm., UT	N < 5	* Gose and Helsley, 1972
Ankareh Fm., WY	rotated	* Grubbs and Van der Voo, 1976
Dunkard Fm., WV	af demag not fully cleaned	* Helsley, 1965
Cutler Fm., CO	N < 5	* Helsley, 1971
Holyoke and Granby Flows, MA	af demag not fully cleaned, only 2 flows, N = 5	* Irving and Banks, 1961
Kayenta Fm., UT	NSM	* Johnson and Nairn, 1972
Luning Fm., NV	NSM	* Kluger-Cohen et al., 1986
Sil Nakya Fm., AZ	NSM	* Kluger-Cohen et al., 1986
Fountain and Lykins Fms., CO	NSM	* McMahon and Strangway, 1968
Upper Maroon Fm., CO	NSM	* McMahon and Strangway, 1968
Minturn and Maroon Fms., CO	NSM	* Miller and Opdyke, 1985
Dewey Lake FM, TX	alpha ratio < 1.15	* Molina-Garza et al., 1989
Bernal Fm., NM	N < 5	* Molina-Garza et al., 1991
Searston Fm., Nfld.	not high-T mag., lies far from path	* Murthy, 1985
Black Prince LS, AZ	NSM	[12]
Gays River host rock, Nova Scotia	alpha ratio < 1.15	[15]
Brush Creek Limestone, PA	NSM	* Payne et al, 1981
Wolfcampian redbeds, AZ, NM, UT	superceded by later studies	* Peterson and Nairn, 1971
Leonardian Toroweap Fm, AZ	N < 5	* Peterson and Nairn, 1971
Hartford and Newark Basins, CT, NJ	only 2 regular flows and 1 anomalous flow	* Prevot and Mc Williams, 1989
Moenkopi Fm., AZ	NSM	* Purucker et al., 1980
Chinle Fm., NM	T-demag not fully cleaned (550°C)	* Reeve and Helsley, 1972
Cutler Fm., UT	N < 5	* Reynolds et al., 1985
Maringouin and Shepody Fms., Nova Scotia	alpha ratio < 1.2	* Roy and Park, 1974
Pictou Group, Nova Scotia	superceded by Pan and Symons, 1993	* Roy, 1966
Morien Group, Nova Scotia	N < 5	* Scotese et al., 1984
Pomquet and Lismore Fms., Nova Scotia	N < 5	* Scotese et al., 1984
Helderberg, NY–VA	syn-folding magnetization	* Scotese, 1985
New Brunswick Volcanics I	pole lies too far from path	* Seguin et al., 1985
Gaspe dikes and contacts, Que.	pole lies too far from path	* Seguin, 1987
Chugwater Fm., WY	N < 5	* Shive et al., 1984
Newark Volcanics, CT-MD	alpha ratio < 1.2	* Smith and Noltimier, 1979
Summerville sandstone, UT	NSM	* Steiner, 1978
Abo Fm., NM	NSM	* Steiner, 1988
Laborcita Fm., NM	NSM	* Steiner, 1988
Wescogame Fm. (Supai), AZ	NSM	* Steiner, 1988
Moat Volcanics, NH	N < 5	* Van Fossen and Kent, 1990
Newark Basin west limb, NJ	NSM	* Van Fossen et al., 1986
Newark Basin east limb, NJ	NSM	* Van Fossen et al., 1986
Newark Basin, PA	alpha ratio < 1.2	* Witte and Kent, 1989

studies that could not be used (Table 2) include those that lack published site or stratigraphic mean directions, or that are based on too few data entries ( $N < 5$ ). The reasons for the exclusion of other studies are also given in Table 2, and may reflect magnetizations that are synfolding, or elongation factors (axial ratio of the ellipse) that are smaller than 1.2, as discussed in more detail below. Also, if a data set had one disparate direction, the aberrant point was removed from the analysis in order not to unduly bias the distribution analysis.

Analyses were performed in direction space to avoid introducing a biased, more favorable outcome. During the Carboniferous–Triassic interval North America was in equatorial positions, so that most paleomagnetic directions are shallow. This means that circularly distributed (Fisherian) directions produce elongated virtual geomagnetic pole distributions. Thus, were we to perform the analysis in pole space, elongations would automatically be produced for North America and these could be misconstrued as being caused by APWP because the elongations would coincidentally happen to be more or less tangential to the APWP for much of this time. It is also worth noting that secular variation presumably causes circularly distributed virtual geomagnetic poles. Such a circular pole distribution translates into an elongated distribution of directions, which, at low paleolatitudes, will produce a maximum axis oriented perpendicular to the APWP. The fact that we find very few maximum axes that are orthogonal to the APWP, as discussed below, means that secular variation may well be a major contributor to the distributions, but not to their elongations.

Bingham statistical analysis of the data set for a given paleopole yields three important parameters: the azimuth of the maximum principal axis of the ellipse, the half angle of the maximum principal axis of the ellipse ( $\alpha_{1-2}$ ), and the half angle of the minimum principal axis of the ellipse ( $\alpha_{1-3}$ ). A normalized half angle ( $\alpha_n$ ) is then calculated as  $\alpha_{1-2}/\alpha_{1-3}$ , and gives the elongation factor (which must be  $> 1.2$  for the result to be included). The three parameters and  $\alpha_n$  are listed for each of the studies in Table 1. Fig. 2, from a study of the Joggins section, Nova Scotia [6], shows an example of an elongated site mean distribution.

All analyses were performed in normal polarity

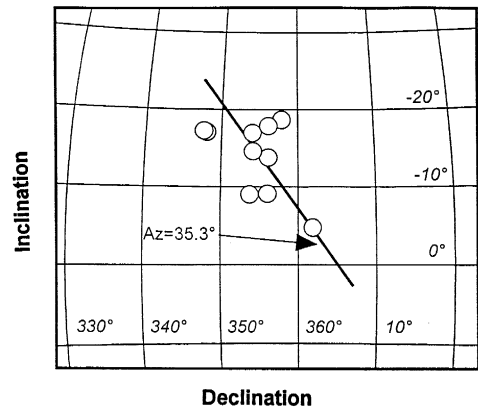


Fig. 2. An example of an elongated directional distribution of site-mean directions. The data are taken from a study of the Joggins section, Nova Scotia [6]. The azimuth is defined in the text and illustrated in Fig. 3.

direction space for the sake of consistency; analyses done on reversed polarity data yield azimuths that are complementary to the azimuths of normal polarity data and this would unnecessarily lead to confusion, a factor overlooked by Lewchuk and Symons [4],

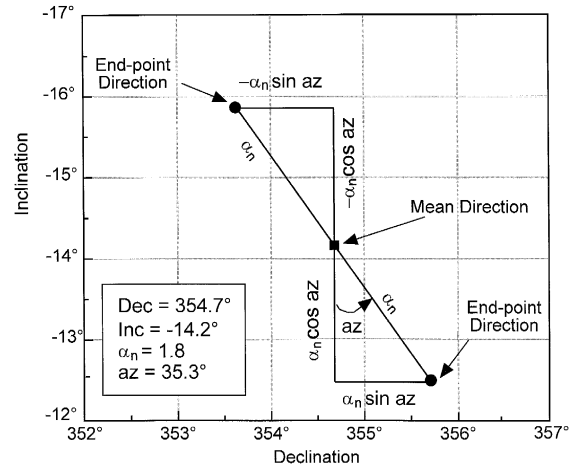


Fig. 3. Determination of the directions of the extremities of the normalized long axis of the Bingham error ellipse to be projected in polar co-ordinates as polar cords. We normalize the elongation of the distributions by calculating the ratio of the major to minor axes ( $\alpha_n$ ) of the error ellipse. The directions of the extremities are then simply calculated using the azimuth of the major axis and the alpha ratio ( $\alpha_n$ ).

who used azimuths of either polarity in their analyses. An azimuth of zero degrees equates to variation purely in inclination while an azimuth of ninety degrees corresponds to variation only in declination.

To plot the polar cords, we calculate directions of the extremities of a distribution, using the mean direction as the center point of the direction–space cord (Fig. 3). The azimuth is measured counterclockwise from the y axis and the length of the cord is  $2\alpha_n$  where  $\alpha_n$  is the normalized half angle, as defined earlier. Thus the declination and inclination values for the extremities are (mean dec +  $\alpha_n \sin az$ , mean inc +  $\alpha_n \cos az$ ) and (mean dec –  $\alpha_n \sin az$ , mean inc –  $\alpha_n \cos az$ ). The extremities are paleomagnetic directions which are then used to calculate the poles that are connected as a polar cord. Strictly speaking, the cord between the two poles at its extremities does not precisely pass through the pole representing the mean direction, as it is a great circle, whereas adding the mean pole probably defines a small circle. However, at the scale at which these cords are plotted, the difference is not noticeable in the figures.

### 3. Results and discussion

Poles of the paleomagnetic data base for the Carboniferous through the Early Jurassic are plotted in Fig. 4. Dots (Fig. 4a) are the paleopoles of the studies used and the circles (Fig. 4b) represent the data that could not be used (Table 2). Based solely upon these plots of the paleopoles, one can already infer that there is a SE–NW trend of the APWP, but we will see below that there is further definition to the APWP. Fig. 5 shows the polar cords: the first three plots include different ranges of  $\alpha_n$ . The orientation of the cords does not appear to depend upon the size of  $\alpha_n$ , provided  $\alpha_n > 1.2$ . Fig. 5d includes all the data used in this study and the improved resolution of the path begins to become apparent. Plots were also generated to test if there was any systematic variation in the orientations of the cords relative to the established APWP [5] for the Carboniferous–Early Jurassic based upon the number of entries per study: no such correlation was found, provided  $N = 5$  or greater.

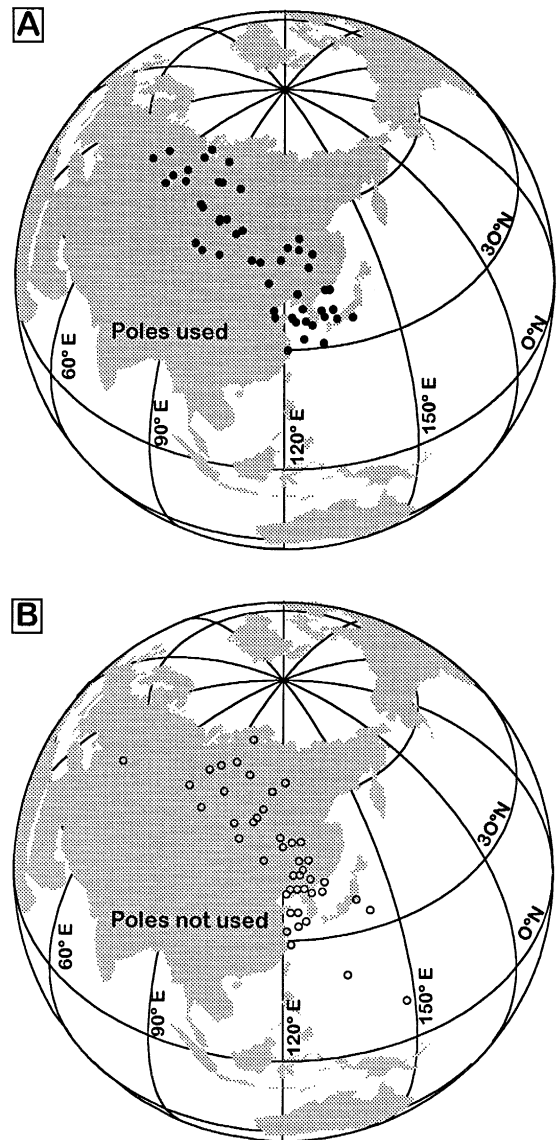


Fig. 4. (a) Carboniferous to Early Jurassic paleopoles from North America from the studies we have used in our analysis (Table 1). (b) Carboniferous to Early Jurassic paleopoles from North America from studies we have not used in our analysis (Table 2). Reasons for the rejection of studies are outlined in the text and Table 2. Both sets of poles define a similar SE–NW trend of APWP.

Fig. 6a is a histogram showing the angular difference between the cords and the tangents to the established APWP [5] (Fig. 6c) nearest the particular

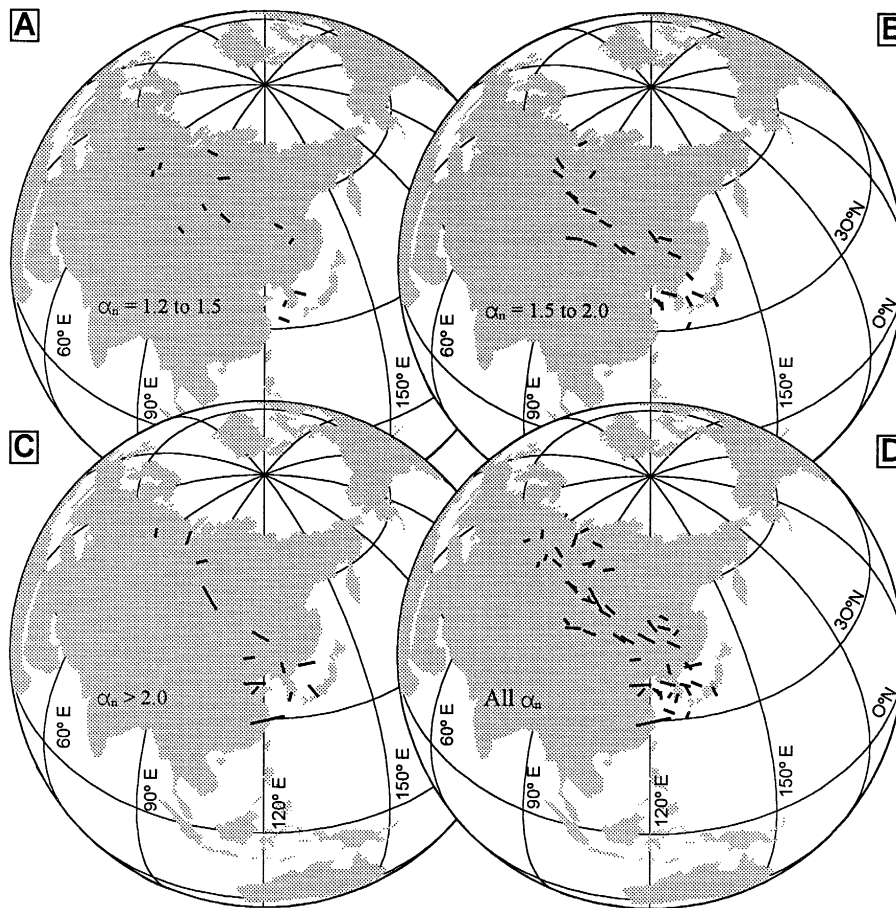


Fig. 5. Plots illustrating the calculated polar cords for varying ranges of  $\alpha_n$ . No obvious differences are noted in the observed trends, indicating that a minimum  $\alpha_n$  of 1.2 is adequate for analyzing the detail in the APWP.

paleopole. Fig. 6 clearly shows that the data are in good agreement with the APWP, particularly in its relatively straight portion representing the Late Permian and Triassic where most polar cords lie sub-parallel to the path (Fig. 6b). Near the sections of the APWP where there are cusps or loops the trends are in less agreement, presumably because the APWP is a smoothed representation of the cusps. Both the Carboniferous bend and the Triassic–Jurassic cusp are characterized by polar cords that show considerable variation in orientation: some trend in the same direction as the Permo–Triassic segment, whereas other cords are perpendicular and appear to follow a smoothly curved path. Some of the cords at the younger end of the APWP suggest that the cusp is

actually quite sharp (as was originally proposed by Gordon et al. [7]). In contrast, other cords near the curved sections of the APWP are probably due to sampling across a length of time which includes both arms of a loop or cusp. The distribution in the histogram (Fig. 6a) reflects this: as the azimuths of the cords are being compared to a smoothed (and somewhat artificial) path, the greater deviations from  $0^\circ$  primarily reflect the trends near the loops of the path. The white swath in Fig. 6c is an approximation of the APWP based on the cords shown and may be compared with a more conventional APWP based on Fisher statistics (e.g., [5]). It is possible to infer from Fig. 6c that an additional switchback exists near the middle–Upper Carboniferous loop, implying a quite

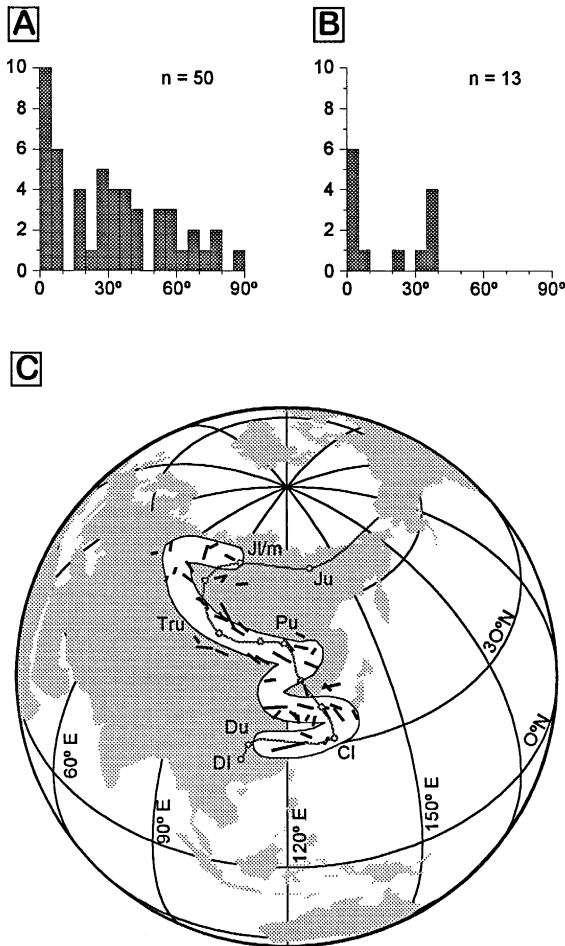


Fig. 6. (a) Histogram illustrating the angular differences between the azimuth calculated from the Bingham statistics and the trend of the APWP of Van der Voo [5]. Angular differences were estimated from the APW trends closest to the polar cord. Over half the azimuths fall within  $30^\circ$  of the trend of the APWP. The greater angular differences are from data points near the cusps of the APWP, where the calculated APWP may represent a smoothing of the true course of APW and the cord may also reflect a sampling of both arms of the cusp. (b) Histogram of a subset of that of (a) for the Late Permian and Triassic straight APWP segment only. (c) The APW path of Van der Voo [5] (thin line connecting circles) for North America for Devonian to Jurassic time plotted along with the polar cords of Fig. 5. The white swath represents an approximation of APW based upon the polar cords. Note that the polar cords suggest a more complicated course of APW in the Carboniferous and may also suggest sharper cusps in the Permian and Late Triassic to Early Jurassic.

convoluted APWP. Speculatively, this may be related to the collision of North America with Gondwana during the Alleghanian Orogeny.

#### 4. Conclusions

When Bingham statistical analysis is applied to paleomagnetic data sets, it can provide very useful insights into the trend of APWPs. As shown in this study, a majority of the paleomagnetic studies from Carboniferous–Jurassic units in North America show elongated distributions. Converting the long axes of these directional distributions into polar cords in pole space can help define an APWP or give additional robustness and detail to a poorly established APWP. The data analyzed herein show that there is generally good agreement between the trends of the polar cords and the corresponding trends of the North American APWP. Additional complexities in the Carboniferous loop of the APWP and a sharper definition of the Triassic–Jurassic cusp can also be surmised from this study. The additional details provided by the use of Bingham statistics can result in a much sharper definition in APWPs and, hence, can lead to improved continental reconstructions.

#### Acknowledgements

We wish to thank Steve Gillett and Craig Jones for providing some of the software for this analysis. Bernard Henry and David Symons provided thorough and thoughtful reviews of the manuscript. [CL]

#### References

- [1] R.A. Fisher, Dispersion on a sphere, Proc. R. Soc. London A, 217, 295–305, 1953.
- [2] C. Bingham, An antipodally symmetric distribution on the sphere, Ann. Stat. 2, 1201–1225, 1974.
- [3] T.C. Onstott, Application of the Bingham distribution function in paleomagnetic studies, J. Geophys. Res. 85, 1500–1510, 1980.
- [4] M. Lewchuk and D.T.A. Symons, Age and duration of Mississippi Valley-type ore-mineralizing events, Geology 23, 233–236, 1995.
- [5] R. Van der Voo, Paleomagnetism of the Atlantic, Tethys and Iapetus Oceans, 411 pp., Cambridge Univ. Press, Cambridge, 1993.
- [6] V.J. DiVenere and N.D. Opdyke, Magnetic polarity stratigraphy and Carboniferous paleopole positions from the Joggins section, Cumberland structural basin, Nova Scotia, J. Geophys. Res. 96, 4051–4064, 1991.
- [7] R.G. Gordon, A. Cox and S. O'Hare, Paleomagnetic Euler poles and the apparent polar wander and absolute motion of

- North America since the Carboniferous, *Tectonics* 3, 499–537, 1984.
- [8] D.R. Bazard and R.F. Butler, Paleomagnetism of the Chinle and Kayenta Formations, New Mexico and Arizona, *J. Geophys. Res.* 96, 9847–9872, 1991.
- [9] R.D. Elmore, D. London, D. Bagley and D. Fruit, Remagnetization by basinal fluids: Testing the hypothesis in the Viola Limestone, southern Oklahoma, *J. Geophys. Res.* 98, 6237–6254, 1993.
- [10] D.V. Kent, P.E. Olsen and W.K. Witte, Late Triassic–earliest Jurassic geomagnetic polarity sequence and paleolatitudes from drill cores in the Newark rift basin, eastern North America, *J. Geophys. Res.* 100, 14965–14998, 1995.
- [11] R.S. Molina-Garza, J.W. Geissman and R. Van der Voo, Paleomagnetism of the Dockum Group (Upper Triassic), northwest Texas: Further evidence for the J-1 cusp in the North America APWP and implications for Colorado Plateau rotation and rate of Triassic APW, *Tectonics* 14, 979–993, 1995.
- [12] K. Nick, K. Xia and R.D. Elmore, Paleomagnetic and petrographic evidence for early magnetization in successive Terra Rossa paleosols, Lower Pennsylvanian Black Prince Limestone, Arizona, *J. Geophys. Res.* 96, 9873–9885, 1991.
- [13] H. Pan, D.T.A. Symons and D.F. Sangster, Paleomagnetism of the Mississippi Valley-type ore and host rocks in the northern Arkansas and Tri-State districts, *Can. J. Earth Sci.* 27, 923–931, 1990.
- [14] H. Pan, D.T.A. Symons and D.F. Sangster, Paleomagnetism of the Gays River zinc–lead deposit, Nova Scotia: Pennsylvanian ore genesis, *Geophys. Res. Lett.* 20, 1159–1162, 1993.
- [15] H. Pan and D.T.A. Symons, Paleomagnetism of the Mississippi Valley-type Newfoundland zinc deposit: Evidence for Devonian mineralization in the northern Appalachians, *J. Geophys. Res.* 98, 22,415–22,427, 1993.
- [16] H. Perroud and R. Van der Voo, Secondary magnetizations from the Clinton-type iron ores of the Silurian Red Mountain Formation, Alabama, *Earth Planet. Sci. Lett.* 67, 391–399, 1984.
- [17] B. Saffer and C. McCabe, Further studies of carbonate remagnetization in the northern Appalachian basin, *J. Geophys. Res.* 97, 4331–4348, 1992.
- [18] C. Stearns and R. Van der Voo, A paleomagnetic reinvestigation of the Upper Devonian Perry Formation: evidence for late Paleozoic remagnetization, *Earth Planet. Sci. Lett.* 86, 27–38, 1987.
- [19] D.T.A. Symons and D.F. Sangster, Paleomagnetic age of the Central Missouri barite deposits and its genetic implications, *Econ. Geol.* 86, 1–12, 1991.
- [20] W.K. Witte, D.V. Kent and P.E. Olsen, Magnetostratigraphy and paleomagnetic poles from Late Triassic–earliest Jurassic strata of the Newark Basin, *GSA Bull.* 103, 1648–1662, 1991.